Numerical comparison of five difference schemes for coupled Klein–Gordon–Schrödinger equations in quantum physics

2007 J. Phys. A: Math. Theor. 40 9125

(http://iopscience.iop.org/1751-8121/40/30/030)

IOP Publishing Journal of Physics A: Mathematical and Theoretical

J. Phys. A: Math. Theor. **40** (2007) 9125–9135 doi:10.1088/1751-8113/40/30/030

Numerical comparison of five difference schemes for coupled Klein–Gordon–Schrödinger equations in quantum physics

Jialin Hong[1], **Shanshan Jiang**[2,3], **Linghua Kong**[4] **and Chun Li**[2,3]

[1] State Key Laboratory of Scientific and Engineering Computing, Institute of Computational Mathematics and Scientific/Engineering Computing (ICMSEC), Academy of Mathematics and System Sciences (AMSS), Chinese Academy of Sciences (CAS), PO Box 2719, Beijing 100080, People's Republic of China
[2] State Key Laboratory of Scientific and Engineering Computing, ICMSEC, AMSS, CAS, PO Box 2719, Beijing 100080, People's Republic of China
[3] Graduate School of the Chinese Academy of Sciences, Beijing 100080, People's Republic of China
[4] Department of Mathematics, University of Science and Technology of China, Hefei, Anhui 230026, People's Republic of China

E-mail: hjl@lsec.cc.ac.cn, jiangss@lsec.cc.ac.cn, konglh@mail.ustc.edu.cn and lichun@lsec.cc.ac.cn

Received 23 March 2007, in final form 25 June 2007
Published 12 July 2007
Online at stacks.iop.org/JPhysA/40/9125

Abstract

In this paper, we compare the classical conservative properties of five difference schemes applied to the coupled Klein–Gordon–Schrödinger equations in quantum physics, and investigate the numerical behaviour of the schemes in the implementation. Numerical results reveal merits and shortcomings of the schemes, and show that all five schemes are stable in the classical conservation laws. In the sense of preservation of classical conservative properties, conservative schemes are better than others.

PACS numbers: 02.60.Jh, 02.60.Lj, 45.20.Jj

(Some figures in this article are in colour only in the electronic version)

1. Introduction

In this paper, we consider the standard coupled Klein–Gordon–Schrödinger (CKGS) equations

$$\begin{cases} \mathrm{i}\partial_t \varphi + \dfrac{1}{2}\partial_{xx}\varphi + u\varphi = 0, \\ \partial_{tt} u - \partial_{xx} u + u - |\varphi|^2 = 0, \end{cases} \tag{1.1}$$

where $\varphi(x,t)$ denotes a complex scalar nucleon field and $u(x,t)$ denotes a real scalar meson field, respectively. Moreover, $\mathrm{i} = \sqrt{-1}$, and we denote the spatial and temporal direction by (x,t), and $x \in \mathcal{R}, t \geqslant 0$. We supplement (1.1) by prescribing the initial-boundary value conditions for $\varphi(x,t)$ and $u(x,t)$ with

$$\begin{aligned} &\varphi|_{t=0} = \varphi_0(x), \qquad u|_{t=0} = u_0(x), \qquad u_t|_{t=0} = u_1(x), \\ &\lim_{|x|\to\infty} |\varphi(x,t)| = 0, \qquad \lim_{|x|\to\infty} u(x,t) = 0, \end{aligned} \tag{1.2}$$

where $\varphi_0(x)$, $u_0(x)$ and $u_1(x)$ are given initial values.

The CKGS equations (1.1)–(1.2) are classical models to describe the interaction between a conservative complex neutron field and a neutral meson Yukawa in the quantum field theory. Theoretical results concerning it can be found in the literature [2, 4, 5] and some numerical methods have been proposed in [1, 3, 6]. The purpose of this paper is to investigate numerically five difference schemes applied to the CKGS equations, especially to compare the preservation of classical conservation laws in numerical implementation.

The outline of the paper is as follows. We review some properties of the CKGS equations in section 2. Some numerical methods are also presented in this section. Then conservation laws are simply investigated in section 3. Finally, some numerical experiments are shown in section 4, and some interesting numerical phenomena are also discovered in this section. Finally, we draw some conclusions to end the paper.

2. Invariants and numerical methods for the CKGS equations

We review some properties of the CKGS equations (1.1) in the section, including charge conservation law, energy conservation law, momentum conservation law and mean value conservation law. Various difference schemes which are all of second order both in time and space are also constructed in this section.

The invariants follow along with the CKGS equations.

(I) Charge conservation law

$$C(t) := \int_{\mathcal{R}} |\varphi(x,t)|^2 \,\mathrm{d}x = \int_{\mathcal{R}} |\varphi_0(x)| := C(0), \quad t \geqslant 0. \tag{2.1}$$

(II) Energy conservation law

$$\begin{aligned} E(t) &:= \int_{\mathcal{R}} (u(x,t)^2 + u_t(x,t)^2 + u_x(x,t)^2 + |\varphi_x(x,t)|^2) - 2u(x,t)|\varphi(x,t)|^2 \,\mathrm{d}x \\ &= \int_{\mathcal{R}} (u(x,0)^2 + u_t(x,0)^2 + u_x(x,0)^2 + |\varphi_x(x,0)|^2) \\ &\quad - 2u(x,0)|\varphi(x,0)|^2 \,\mathrm{d}x := E(0). \end{aligned} \tag{2.2}$$

(III) Momentum conservation law

$$\begin{aligned} M(t) &:= \int_{\mathcal{R}} \mathcal{I}m(\overline{\varphi}(x,t)\varphi_x(x,t)) - u_t(x,t)u_x(x,t) \,\mathrm{d}x \\ &= \int_{\mathcal{R}} \mathcal{I}m(\overline{\varphi}(x,0)\varphi_x(x,0)) - u_t(x,0)u_x(x,0) \,\mathrm{d}x = M(0), \end{aligned} \tag{2.3}$$

where '$\mathcal{I}m$' denotes the imaginary part, and $\overline{\varphi}$ denotes the complex conjugate of φ.

(IV) Mean value conservation law

$$N(t) = C(0) + (\widetilde{N}(u_0) - C(0))\cos(t) + \widetilde{N}(u_1)\sin(t) = N(0), \tag{2.4}$$

where $N(t) := \widetilde{N}(u(\cdot,t)) = \int_{\mathcal{R}} u(x,t) \,\mathrm{d}x$.

These are formal invariants of the CKGS equations. Naturally, the most interesting thing is to search for effective schemes to preserve these formal invariants as much as possible. Thus, it motivates us to investigate their various numerical schemes, and compare their numerical results. We list five difference schemes for the CKGS equations and compare their numerical phenomena.

We choose h and τ as the spatial mesh grid size and the temporal step size, respectively. For convenience, we introduce a uniform grid $(x_j, t_k) \in \mathcal{R} \times R^+$. The approximation of the value of the function $V(x,t)$ at the mesh grid (x_j, t_k) is denoted by V_j^k. The concrete schemes are the following.

Scheme (M-M). This is constructed by applying the implicit midpoint method to both directions of equations in [3]

$$\mathrm{i}\big(\delta_t\varphi_{j+1/2}^{n+1/2}+\delta_t\varphi_{j-1/2}^{n+1/2}\big)+\delta_x^2\varphi_j^{n+1/2}+\big(\varphi_{j+1/2}^{n+1/2}u_{j+1/2}^{n+1/2}+\varphi_{j-1/2}^{n+1/2}u_{j-1/2}^{n+1/2}\big)=0,$$

$$\big(\delta_t^2u_{j+1/2}^n+\delta_t^2u_{j-1/2}^n\big)-\big(\delta_x^2u_j^{n+1/2}+\delta_x^2u_j^{n-1/2}\big)+\tfrac{1}{2}\big(u_{j+1/2}^{n+1/2}+u_{j-1/2}^{n+1/2}+u_{j+1/2}^{n-1/2}+u_{j-1/2}^{n-1/2}\big)-\tfrac{1}{2}\big(\big|\varphi_{j+1/2}^{n+1/2}\big|^2+\big|\varphi_{j-1/2}^{n+1/2}\big|^2+\big|\varphi_{j+1/2}^{n-1/2}\big|^2+|\varphi_{j-1/2}^{n-1/2}|^2\big)=0,$$

where $\varphi_{j+1/2}^{n+1/2}=\frac{1}{2}\big(\varphi_{j+1/2}^{n+1}+\varphi_{j+1/2}^{n}\big)=\frac{1}{2}\big(\varphi_{j+1}^{n+1/2}+\varphi_{j}^{n+1/2}\big)=\frac{1}{4}\big(\varphi_{j+1}^{n+1}+\varphi_{j+1}^{n}+\varphi_{n+1}^{j}+\varphi_j^n\big)$, $\delta_t\varphi_{j+1/2}^{n+1/2}=\frac{\varphi_{j+1/2}^{n+1}-\varphi_{j+1/2}^{n}}{\tau}$, $\delta_t^2u_{j+1/2}^n=\frac{u_{j+1/2}^{n+1}-2u_{j+1/2}^n+u_{j+1/2}^{n-1}}{\tau^2}$, $\delta_x^2u_j^{n+1/2}=\frac{u_{j+1}^{n+1/2}-2u_j^{n+1/2}+u_{j-1}^{n+1/2}}{h^2}$, etc. This scheme was proved to be multisymplectic [3].

Scheme (M-C). This applies the implicit midpoint method to the t-direction and central difference method to the x-direction:

$$\mathrm{i}\delta_t\varphi_j^{n+1/2}+\tfrac{1}{4}\big(\delta_x^2\varphi_j^{n+1}+\delta_x^2\varphi_j^n\big)+u_j^{n+1/2}\varphi_j^{n+1/2}=0,$$

$$\delta_t^2u_j^n-\tfrac{1}{4}\big(\delta_x^2u_j^{n-1}+2\delta_x^2u_j^n+\delta_x^2u_j^{n+1}\big)+\tfrac{1}{2}\big(u_j^{n-1/2}+u_j^{n+1/2}\big)-\tfrac{1}{2}\big(\big|\varphi_j^{n-1/2}\big|^2+\big|\varphi_j^{n+1/2}\big|^2\big)=0.$$

Scheme (T-C). This is constructed by applying the trapezoidal method to the t-direction and central difference method to the x-direction:

$$\mathrm{i}\delta_t\varphi_j^{n+1/2}+\tfrac{1}{4}\big(\delta_x^2\varphi_j^{n+1}+\delta_x^2\varphi_j^n\big)+\tfrac{1}{2}\big(u_j^{n+1}\varphi_j^{n+1}+u_j^n\varphi_j^n\big)=0,$$

$$\delta_t^2u_j^n-\tfrac{1}{2}\big(\delta_x^2u_j^{n-1/2}+\delta_x^2u_j^{n+1/2}\big)+\tfrac{1}{2}\big(u_j^{n-1/2}+u_j^{n+1/2}\big)-\tfrac{1}{4}\big(\big|\varphi_j^{n+1}\big|^2+2\big|\varphi_j^n\big|^2+\big|\varphi_j^{n-1}\big|^2\big)=0.$$

Scheme (T-T). This is constructed by applying the trapezoidal method to both directions of equations

$$\mathrm{i}\big(\delta_t\varphi_{j+1}^{n+1/2}+2\delta_t\varphi_j^{n+1/2}+\delta_t\varphi_{j-1}^{n+1/2}\big)+\big(\delta_x^2\varphi_j^{n+1}+\delta_x^2\varphi_j^n\big)+\tfrac{1}{2}\big(u_{j+1}^{n+1}\varphi_{j+1}^{n+1}+2u_j^{n+1}\varphi_j^{n+1}+u_{j-1}^{n+1}\varphi_{j-1}^{n+1}+u_{j+1}^n\varphi_{j+1}^n+2u_j^n\varphi_j^n+u_{j-1}^n\varphi_{j-1}^n\big)=0,$$

$$\big(\delta_t^2u_{j+1}^n+\delta_t^2u_j^n+\delta_t^2u_{j-1}^n\big)-\big(\delta_x^2u_j^{n+1}+\delta_x^2u_j^n+\delta_x^2u_j^{n-1}\big)+(u_{j+1/2}^{n+1/2}+u_{j+1/2}^{n-1/2}+u_{j-1/2}^{n+1/2}+u_{j-1/2}^{n-1/2})-\tfrac{1}{4}\big[\big|\varphi_{j+1}^{n+1}\big|^2+2\big|\varphi_j^{n+1}\big|^2+\big|\varphi_{j-1}^{n+1}\big|^2+2\big(\big|\varphi_{j+1}^n\big|^2+2\big|\varphi_j^n\big|^2+\big|\varphi_{j-1}^n\big|^2\big)+\big|\varphi_{j+1}^{n-1}\big|^2+2\big|\varphi_j^{n-1}\big|^2+\big|\varphi_{j-1}^{n-1}\big|^2\big]=0.$$

Conservative scheme (C-C). This was proposed by Zhang [6]:

$$\mathrm{i}\delta\varphi_j^{n+1/2}+\tfrac{1}{4}\big(\delta_x^2\varphi_j^{n+1}+\delta_x^2\varphi_j^n\big)+\tfrac{1}{4}\big(u_j^n+u_j^{n+1}\big)\big(\varphi_j^n+\varphi_j^{n+1}\big)=0,$$

$$\delta_x^2u_j^n-\delta_x^2u_j^n+\tfrac{1}{2}\big(u_j^{n+1}+u_j^{n-1}\big)-|\varphi_j^n|^2=0.$$

We would like to emphasize here that all the five schemes are implicit since all of them, applied to the nonlinear equations, need iterative process from time t_k to t_{k+1}, and the differences among the schemes (M-M), (T-T), (M-C) and (T-C) are in the discretization of the nonlinear terms.

In the subsequent section, we investigate the discrete conservative quantities of the five difference schemes.

3. Discrete conservation laws of the difference schemes

In this section, we study the discrete conservation laws of the difference schemes presented in the previous section.

Lemma 3.1. *Both schemes (C-C) and (T-C) possess the discrete charge conservation law, i.e.,*

$$h\sum_j |\varphi_j^k|^2 = h\sum_j |\varphi_j^0|^2, \tag{3.1}$$

where $\varphi_j^0 = \varphi_0(x_j)$ *is the initial value.*

We refer to [6] for the proof of this lemma.

Lemma 3.2 ([3])**.** *The scheme (M-M) admits the discrete charge conservation law, i.e.*

$$h\sum_j \left|\frac{\varphi_j^k + \varphi_{j+1}^k}{2}\right|^2 = h\sum_j \left|\frac{\varphi_j^0 + \varphi_{j+1}^0}{2}\right|^2. \tag{3.2}$$

Lemma 3.3 ([6])**.** *The scheme (C-C) satisfies the discrete energy conservation law in the following sense:*

$$E^n = E^{n-1} = \cdots = E^0, \tag{3.3}$$

where

$$E^n = h\sum_j \left|\frac{\varphi_{j+1}^{n+1} - \varphi_j^{n+1}}{h}\right|^2 + h\sum_j \left|\frac{u_j^{n+1} - u_j^n}{\tau}\right|^2 + h\sum_j \frac{u_{j+1}^n - u_j^n}{h}\frac{u_{j+1}^{n+1} - u_j^{n+1}}{h}$$
$$+ \frac{1}{2}h\sum_j \left(|u_j^{n+1}|^2 + |u_j^n|^2\right) - h\sum_j \left(u_j^{n+1} + u_j^n\right)|\varphi_j^{n+1}|^2,$$

which is an approximation of the energy conservation law (2.2).

The other four schemes cannot preserve the discrete energy conservation laws exactly. But we can investigate their residuals numerically. Furthermore, the truncation errors of the above five schemes reach $\mathcal{O}(\tau^2 + h^2)$, which can be easily verified by Taylor expansion.

4. Numerical experiments

In this section, we carry out some numerical experiments to observe the numerical phenomena by using the five difference schemes presented in the previous section.

For the convenience of comparisons, we give some solitary-wave solutions of the CKGS equations (1.1),

$$\begin{cases} \varphi(x,t,q) = \dfrac{3\sqrt{2}}{4\sqrt{1-q^2}}\operatorname{sech}^2\dfrac{1}{2\sqrt{1-q^2}}(x - qt - x_0)\exp\left(\mathrm{i}\left(qx + \dfrac{1-q^2+q^4}{2(1-q^2)}t\right)\right), \\ u(x,t,q) = \dfrac{3}{4(1-q^2)}\operatorname{sech}^2\dfrac{1}{2\sqrt{1-q^2}}(x - qt - x_0), \end{cases} \tag{4.1}$$

where q $(0 \leqslant |q| < 1)$ indicates the propagating velocity of wave, x_0 is the initial phase.

The initial values

$$\varphi_0(x) = \varphi(x,0,q), \qquad u_0(x) = u(x,0,q), \qquad v_0(x) = u_t(x,t,q)|_{t=0}$$

are obtained from (4.1) as $t = 0$.

Table 1. Errors between numerical solutions and analytic solutions.

$\tau \setminus h$	method	L^∞ error of u	L^2 error of u	L^∞ error of φ	L^2 error of φ
0.1\0.2	M-M	$3.404\,209 \times 10^{-4}$	$3.341\,671 \times 10^{-3}$	$5.032\,287 \times 10^{-3}$	$6.402\,466 \times 10^{-3}$
	M-C	$8.853\,035 \times 10^{-4}$	$1.271\,846 \times 10^{-3}$	$1.964\,584 \times 10^{-3}$	$3.053\,696 \times 10^{-3}$
	T-C	$1.196\,352 \times 10^{-3}$	$1.366\,835 \times 10^{-3}$	$2.059\,972 \times 10^{-3}$	$3.174\,964 \times 10^{-3}$
	T-T	$1.477\,323 \times 10^{-3}$	$2.750\,816 \times 10^{-3}$	$4.483\,451 \times 10^{-3}$	$6.540\,302 \times 10^{-3}$
	C-C	$1.258\,607 \times 10^{-3}$	$1.424\,779 \times 10^{-3}$	$2.078\,082 \times 10^{-3}$	$3.134\,800 \times 10^{-3}$
0.05\0.1	M-M	$9.515\,770 \times 10^{-5}$	$8.840\,607 \times 10^{-4}$	$1.335\,464 \times 10^{-3}$	$1.693\,839 \times 10^{-3}$
	M-C	$2.350\,719 \times 10^{-4}$	$3.387\,470 \times 10^{-4}$	$5.078\,567 \times 10^{-4}$	$8.004\,568 \times 10^{-4}$
	T-C	$3.163\,652 \times 10^{-4}$	$3.636\,545 \times 10^{-4}$	$5.341\,095 \times 10^{-4}$	$8.328\,130 \times 10^{-4}$
	T-T	$3.911\,607 \times 10^{-4}$	$7.221\,917 \times 10^{-4}$	$1.178\,744 \times 10^{-3}$	$1.701\,153 \times 10^{-3}$
	C-C	$3.325\,115 \times 10^{-4}$	$3.784\,952 \times 10^{-4}$	$5.392\,754 \times 10^{-4}$	$8.222\,223 \times 10^{-4}$
0.025\0.05	M-M	$2.500\,168 \times 10^{-5}$	$2.269\,768 \times 10^{-4}$	$3.420\,941 \times 10^{-4}$	$4.347\,211 \times 10^{-4}$
	M-C	$6.063\,758 \times 10^{-5}$	$8.729\,277 \times 10^{-5}$	$1.292\,030 \times 10^{-4}$	$2.045\,860 \times 10^{-4}$
	T-C	$8.134\,725 \times 10^{-5}$	$9.368\,392 \times 10^{-5}$	$1.358\,407 \times 10^{-4}$	$2.129\,327 \times 10^{-4}$
	T-T	$1.011\,365 \times 10^{-4}$	$1.854\,060 \times 10^{-4}$	$3.002\,562 \times 10^{-4}$	$4.341\,851 \times 10^{-4}$
	C-C	$8.563\,031 \times 10^{-5}$	$9.742\,859 \times 10^{-5}$	$1.371\,329 \times 10^{-4}$	$2.102\,248 \times 10^{-4}$

4.1. Solitary wave tests

In order to process numerical investigations, we choose $x_0 = -20, q = 0.3$, set the spatial domain $[-L, L]$ and the zero boundary conditions

$$\varphi(-L, t) = \varphi(L, t) = 0, \qquad u(-L, t) = u(L, t) = 0.$$

During the subsequent practical computation, we choose $L = 40$.

Furthermore, errors between numerical solutions and analytic solutions in sense of L^2 and L^∞ norms are, respectively, defined as

$$\left\|\text{error}_\varphi^n\right\|_2 = \left(h \sum_j |\varphi(x_j, t_n) - \varphi_j^n|^2\right)^{\frac{1}{2}}, \qquad \left\|\text{error}_\varphi^n\right\|_\infty = \max_j \left|\varphi(x_j, t_n) - \varphi_j^n big\right|. \tag{4.2}$$

Table 1 shows errors for the five difference schemes at $T = 1$. From the two tables, we can conclude numerically that the numerical results are consistent with the theoretical ones that the numerical solutions u, φ are of order $\mathcal{O}(\tau^2 + h^2)$.

The corresponding approximations of (2.1), (2.2) and (2.3) at $t = t_n$ are denoted by C^n, E^n and M^n, respectively, and the residual of the charge at t_n is given by $C^n - C^0$, so do the energy and momentum.

For the purpose of illustrations and comparisons, we give their numerical behaviour in the time interval [0, 100] with various temporal and spatial step-sizes. The numerical results are presented in figures 1–3.

Figure 1 presents the residuals of energy E^n. Except for scheme (C-C) preserving the energy conservation law exactly in the scale of 10^{-12}, all the other four schemes exhibit the similar changes: the residuals are reduced to about $\frac{1}{16}$ roughly, as both the spatial mesh grid size and the temporal step size are reduced to $\frac{1}{2}$ simultaneously. And all graphs show oscillation of small amplitude, and no evident fluctuation for a long time. But scheme (T-T) is inferior to the others.

Figure 2 shows the residuals of momentum M^n. All the five schemes cannot preserve the momentum conservation law exactly. Schemes (M-M) and (T-T) exhibit analogous

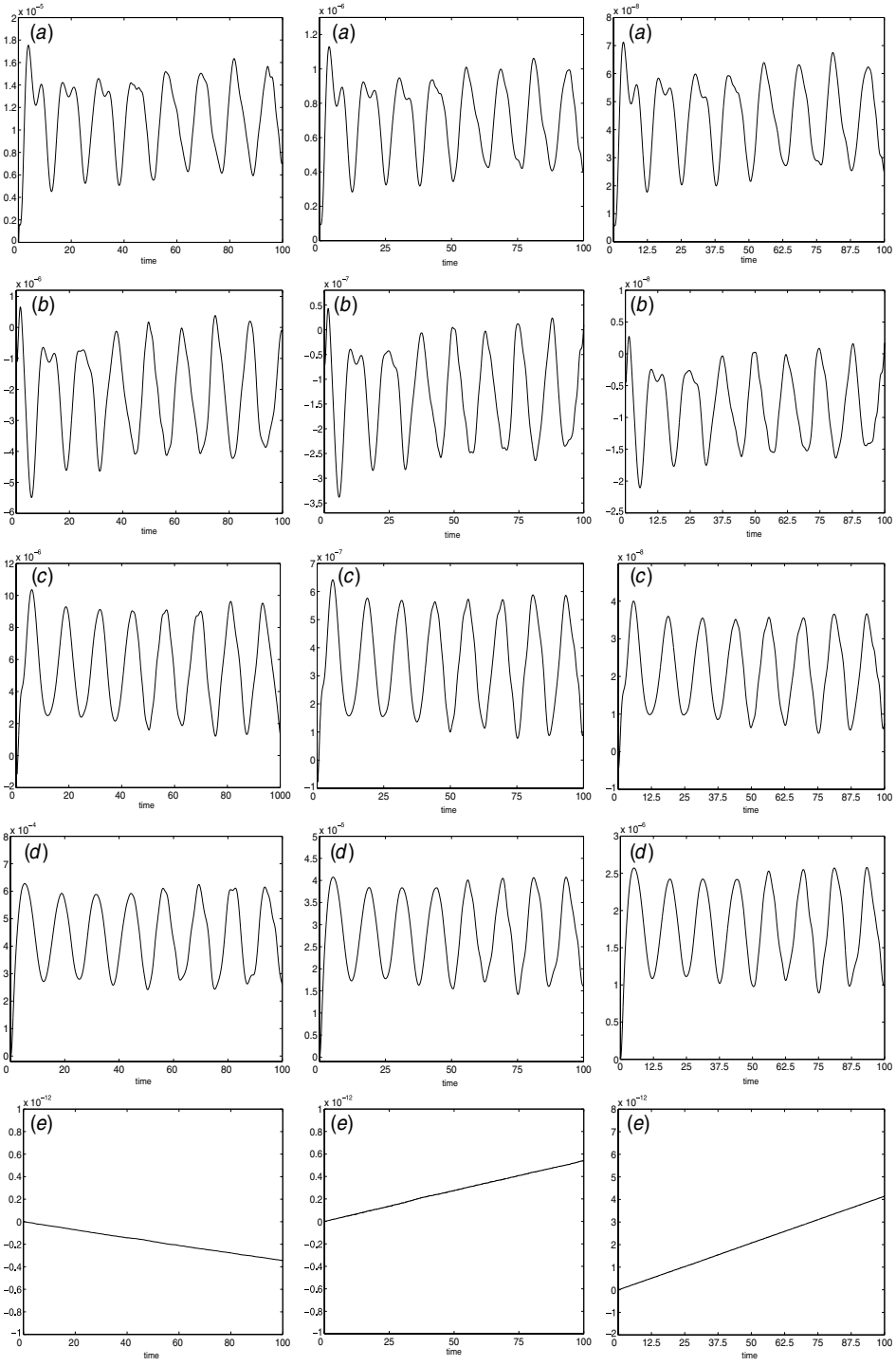

Figure 1. Residuals of energy conservation law with various spatial and temporal step sizes. Left for $\tau = 0.1$ and $h = 0.2$; mid for $\tau = 0.05$ and $h = 0.1$; right for $\tau = 0.025$ and $h = 0.05$; for (*a*) scheme M-M, (*b*) scheme M-C, (*c*) scheme T-C, (*d*) scheme T-T, (*e*) scheme C-C.

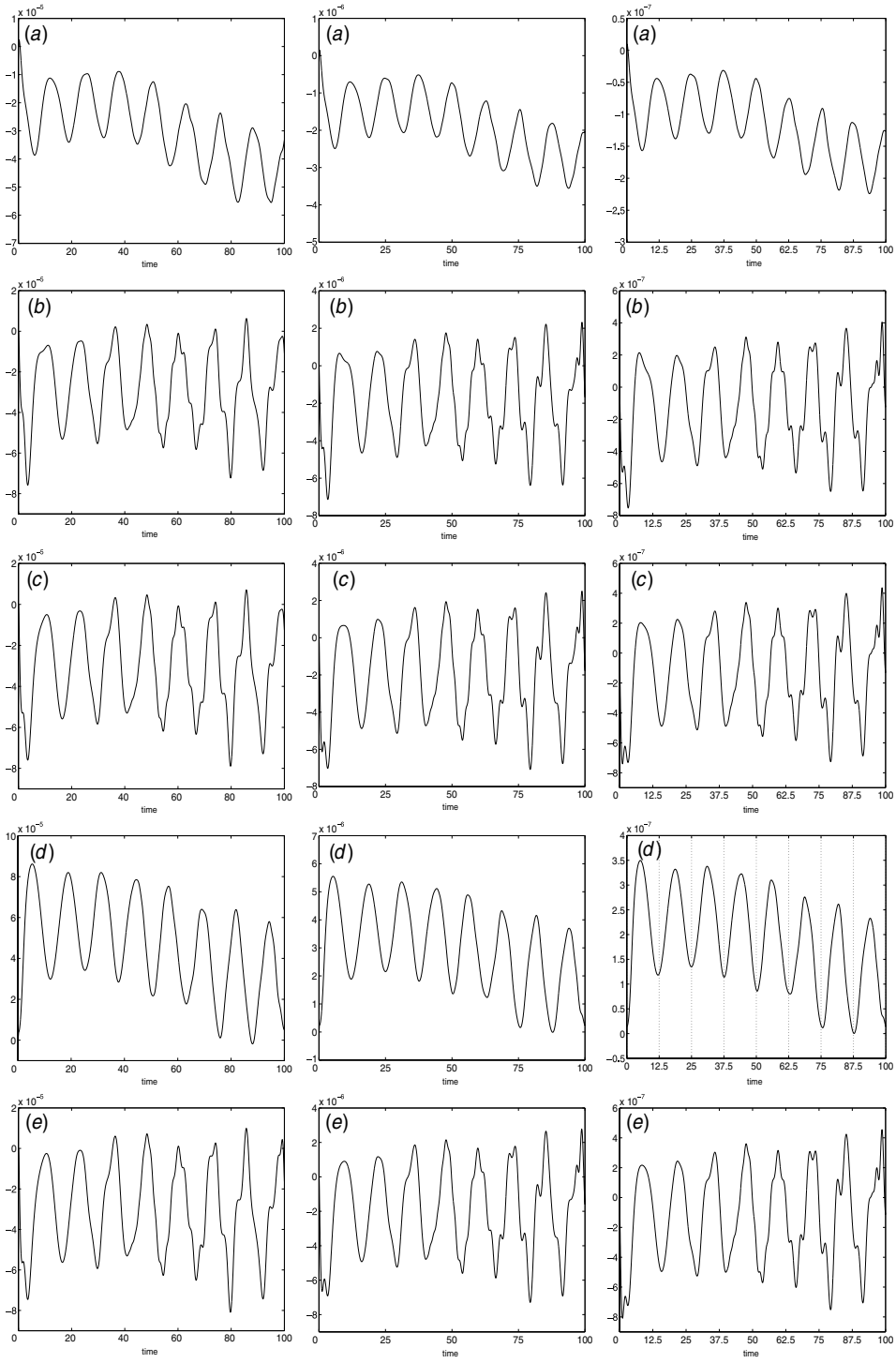

Figure 2. Residuals of momentum conservation law with various spatial and temporal step sizes. Left for $\tau = 0.1$ and $h = 0.2$; mid for $\tau = 0.05$ and $h = 0.1$; right for $\tau = 0.025$ and $h = 0.05$; for (*a*) scheme M-M, (*b*) scheme M-C, (*c*) scheme T-C, (*d*) scheme T-T, (*e*) scheme C-C.

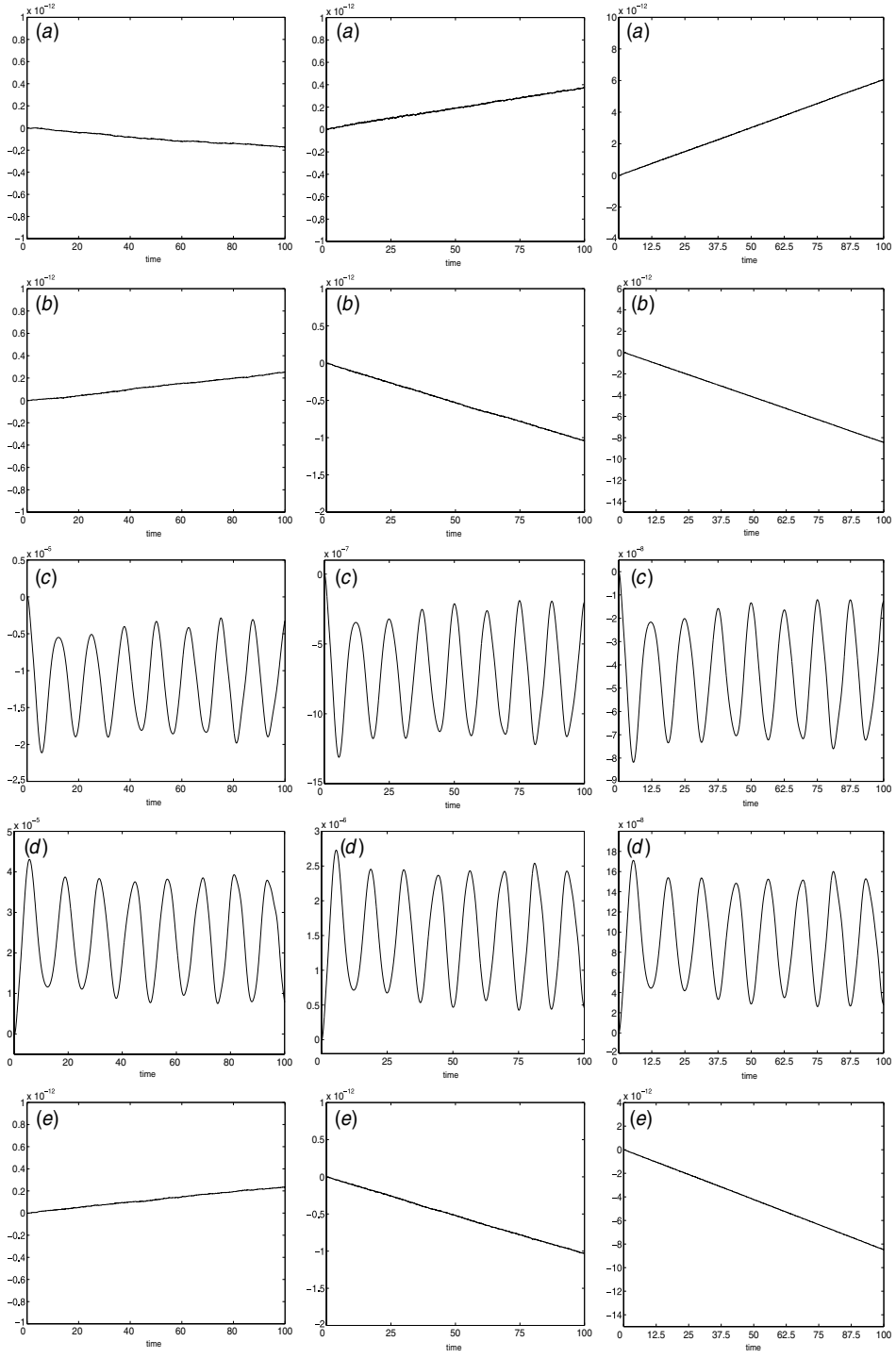

Figure 3. Residuals of charge conservation law with various spatial and temporal step sizes. Left for $\tau = 0.1$ and $h = 0.2$; mid for $\tau = 0.05$ and $h = 0.1$; right for $\tau = 0.025$ and $h = 0.05$; for (*a*) scheme M-M, (*b*) scheme M-C, (*c*) scheme T-C, (*d*) scheme T-T, (*e*) scheme C-C.

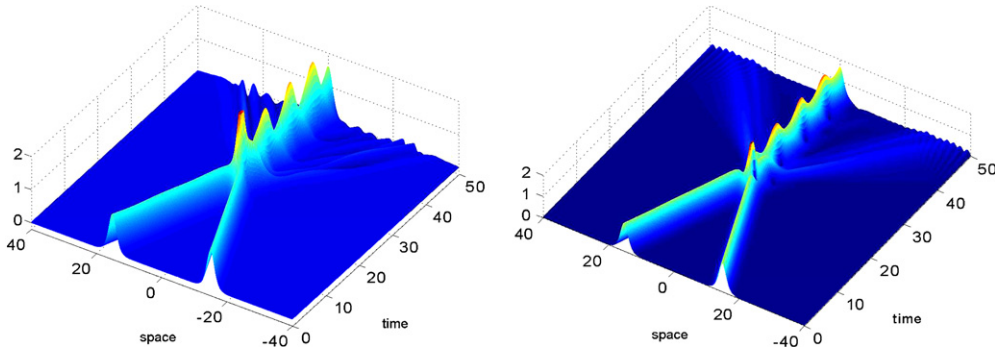

Figure 4. numerical solutions of symmetric collision for scheme (M-M). Left for u, right for $|\varphi|$.

performance along with the increase of time, and the errors are reduced to about $\frac{1}{16}$ roughly, as both of the spatial mesh grid size and the temporal step size are reduced to $\frac{1}{2}$. Schemes (M-C), (T-C) and (C-C) exhibit analogous performance likewise, they have the similar scope of errors.

Figure 3 displays the residuals of charge C^n. We can observe that schemes (M-M), (M-C) and (C-C) all preserve the charge conservation law exactly, which are all in the magnitude of 10^{-12}. These are consistent with the theoretical results in lemma 3.1 and lemma 3.2. Though schemes (T-C) and (T-T) cannot preserve the charge conservation law exactly, they remain the errors in good magnitudes and have no evident increase for a long time with different mesh grid sizes and time step sizes. Moreover, the residuals are in accordance with the rule that they are increased to about 16 times roughly, as both the mesh grid size and the time step size are densified two times.

It can be seen from the experiments that in the case of solitary-wave solutions, all the five schemes are stable in the sense of the energy, charge and momentum conservation laws.

4.2. Collision of solitons

Now, we turn our attentions to the collision of two solitons. The corresponding initial values are chosen as follows:

$$\begin{aligned}
\varphi_0(x) &= \varphi_0(x - x_1, 0, q_1) + \varphi_0(x - x_2, 0, q_2),\\
u_0(x) &= u_0(x - x_1, 0, q_1) + u_0(x - x_2, 0, q_2),\\
v_0(x) &= \{u_t(x - x_1, t, q_1) + u_t(x - x_2, t, q_2)\}|_{t=0},
\end{aligned}$$

where x_1, x_2 are initial phases and q_1, q_2 are propagating velocities of two solitons, respectively.

We choose collision of two solitons with identical speeds and opposite directions (symmetric collision): $x_1 = -15, x_2 = 15$ and $q_1 = 0.6, q_2 = -0.6$, respectively. We solve the problem with the five schemes in the spatial domain $[-40, 40]$ till $T = 50$. In this case, we take $\tau = 0.01$ and $h = 0.2$.

Figure 4 shows the evolution of the solitons calculated by scheme (M-M) as an example. We can find that the two solitons stay at the same position at time around $t = 22.5$, and the solitons keep in this state. After that, the collision results in fusion accompanied by a series of emission of waves.

In figure 5, we give the residuals of energy, momentum and charge for the collision of the two solitons. It can be observed from the longitudinal (left) graphs that the error of energy conservation law is in the scale of 10^{-11} for scheme (C-C) because it is an energy-preserving

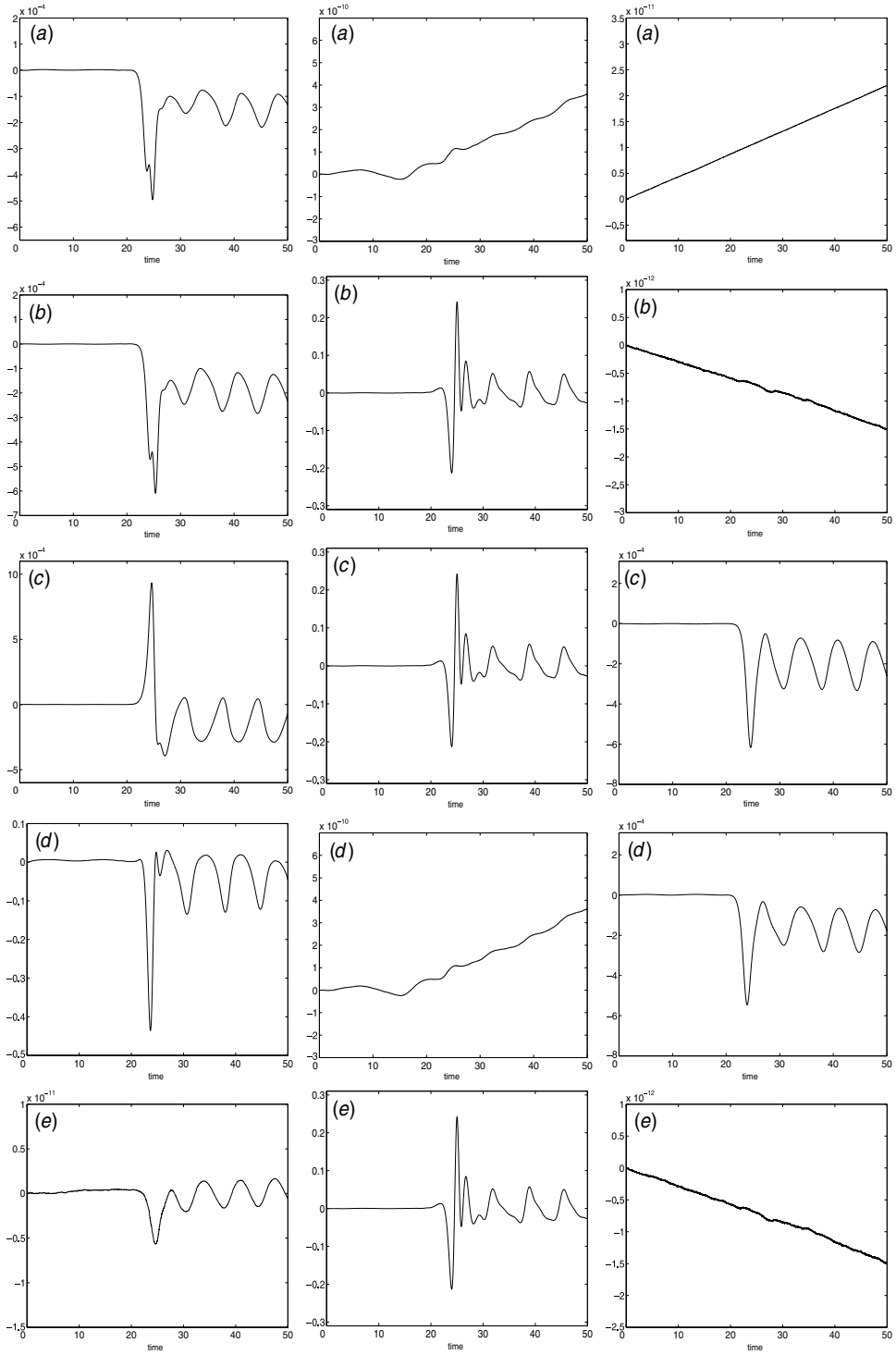

Figure 5. Residuals of energy (left), momentum (mid) and charge (right) conservation law for collision: (*a*) scheme M-M, (*b*) scheme M-C, (*c*) scheme T-C, (*d*) scheme T-T, (*e*) scheme C-C.

scheme, while for schemes (M-M), (M-C) and (T-C) in the scale of 10^{-4}, for scheme (T-T) even in the scale of 10^{-1}. And the errors change larger during collision than others, and exhibit pretty performance with oscillation of little amplitude around some equilibrium state, and have no evident amplification for a long time before and after collision for all the schemes. The longitudinal (mid) graphs exhibit the corresponding errors of the momentum for collision of the two solitons, and we can learn from them that schemes (M-C), (T-C) and (C-C) present the similar performance: the errors change larger during collision, and exhibit pretty performance with oscillation of little amplitude around some equilibrium state, and have no any evident amplification for a long time after collision. But, as a whole, the errors are in the scale of 10^{-1}, and much larger than in the case of solitary wave. Surprisingly, the results of schemes (M-M) and (T-T) are much better than they are expected, which are in the scale of 10^{-10}. Now, turn our eyes to the right, we find that schemes (M-M), (M-C) and (C-C) preserve the charge conservation law exactly, which are in the magnitude of 10^{-12}. But schemes (T-C) and (T-T) are in the scale of 10^{-4}, and the errors change larger during collision, and exhibit pretty performance with oscillation of little amplitude around some equilibrium state, and have no any evident amplification for a long time after collision as other invariant quantities.

In all, though in the case of collision of solitons, all the five schemes remain stable for the energy, charge and momentum conservation laws.

5. Conclusions

We present five difference schemes to simulate the CKGS equations, and investigate their properties numerically, including the discrete energy, charge and momentum conservation laws. The five difference schemes are all of order $\mathcal{O}(\tau^2 + h^2)$. Scheme (C-C) can preserve both the discrete charge and energy conservation laws exactly, and schemes (M-M), (M-C) preserve the discrete charge conservation law exactly, whereas none of them can preserve the discrete momentum conservation law exactly. In sum, scheme (C-C) is superior to schemes (M-M) and (M-C), and the latter two are exceed to schemes (T-C) and (T-T). But sometimes schemes (M-M) and (T-T) can simulate the discrete momentum conservation law precisely.

Acknowledgments

J Hong, S Jiang and C Li are supported by the Director Innovation Foundation of ICMSEC and AMSS, the Foundation of CAS, the NNSFC (no.19971089, no.10371128) and the Special Funds for Major State Basic Research Projects of China 2005CB321701; L Kong is supported by the 2005 postgraduate innovational foundation of USTC.

References

[1] Bao W and Yang L 2007 Efficient and accurate numerical methods for the Klein–Gordon–Schrödinger equations *J. Comput. Phys.* (at press)

[2] Fukuda I and Tsutsumi M 1975 On the Uukawa-coupled Klein–Gordon–Schrödinger equations in three space dimensions *Prof. Japan Acad.* **51** 402–5

[3] Kong L, Liu R and Xu Z 2006 Numerical simulation of interaction between Schrödinger field and Klein–Gordon field by multisymplectic method *Appl. Math. Comput.* **181** 342–50

[4] Ohta M 1996 Stability of stationary states for the coupled Klein–Gordon–Schrödinger equations *Non. Anal.* **27** 455–61

[5] Ozawa T and Tsutsumi Y 1994 Asymptotic behaviour of solutions for the coupled Klein–Gordon–Schrödinger equations *Adv. Stud. Pure Math.* **23** 295–305

[6] Zhang L 2005 Convergence of a conservative difference scheme for a class of Klein–Gordon–Schrödinger equations in one space dimension *Appl. Math. Comput.* **163** 343–55